Determination of the collision cross sections of cardiolipins and phospholipids from Pseudomonas aeruginosa by traveling wave ion mobility spectrometry-mass spectrometry using a novel correction strategy

Estelle Deschamps, Isabelle Schmitz-Afonso, Annick Schaumann, Emmanuelle Dé, Corinne Loutelier-Bourhis, Stephane Alexandre, Carlos Afonso

Determination of the collision cross sections of cardiolipins and phospholipids from *Pseudomonas aeruginosa* by traveling wave ion mobility spectrometry-mass spectrometry using a novel correction strategy

Estelle Deschamps[1,2], Isabelle Schmitz-Afonso[1], Annick Schaumann[2], Emmanuelle Dé[2], Corinne Loutelier-Bourhis[1], Stéphane Alexandre[2], Carlos Afonso[1]

1 Normandie Univ, COBRA, UMR 6014 and FR 3038, Université de Rouen, INSA de Rouen, CNRS, IRCOF, 1 rue Tesnière, 76821 Mont-Saint-Aignan Cedex, France

2 Normandie Univ, PBS, UMR 6270 and FR 3038, Université de Rouen, INSA de Rouen, CNRS, CURIB, 25 Rue Lucien Tesnière, 76821 Mont-Saint-Aignan Cedex, France

Corresponding authors :

* Estelle Deschamps estelle.deschamps@etu.univ-rouen.fr

* Corinne Loutelier-Bourhis corinne.loutelier@univ-rouen.fr

Keywords: Ion mobility spectrometry, Mass spectrometry, *Pseudomonas aeruginosa*, Cardiolipins, Phospholipids, CCS calibration

Received: 22 July 2019 / Revised: 16 September 2019 / Accepted: 7 October 2019 / Published online: 27 November 2019

ABSTRACT

Collision Cross Section (CCS) values are descriptors of the 3D structure of ions which can be determined by ion mobility spectrometry (IMS). Currently, most lipidomic studies involving CCS values determination concerns eukaryote samples (*e.g.* human, bovine) and to a lower extent prokaryote samples (*e.g.* bacteria). Here, we report CCS values obtained from Traveling Wave Ion Mobility spectrometry ($^{TW}CCS_{N2}$) measurements from the bacterial membrane of *Pseudomonas aeruginosa* - a bacterium ranked as priority 1 for the R&D of new antibiotics by the World Health Organization. In order to cover the lack of reference compounds which could cover the *m/z* and CCS range of the membrane lipids of *P. aeruginosa*, three calibrants (polyalanine, dextran and phospholipids) were used for the $^{TW}CCS_{N2}$ calibration. A shift from the published lipids CCS values was systematically observed (ΔCCS% up to 9%), thus we proposed a CCS correction strategy. This correction strategy allowed to reduce the shift (ΔCCS%) between our measurements and published values to less than 2%. This correction was then applied to determine the CCS values of *Pseudomonas aeruginosa* lipids which have not been published yet. As a result, 32 $^{TW}CCS_{N2}$ values for $[M+H]^+$ ions and 24 $^{TW}CCS_{N2}$ values for $[M-H]^-$ ions were obtained for four classes of phospholipids (phosphatidylethanolamines (PE), phosphatidylcholines (PC), phosphatidylglycerols (PG) and diphosphatidylglycerols —known as cardiolipins (CL)).

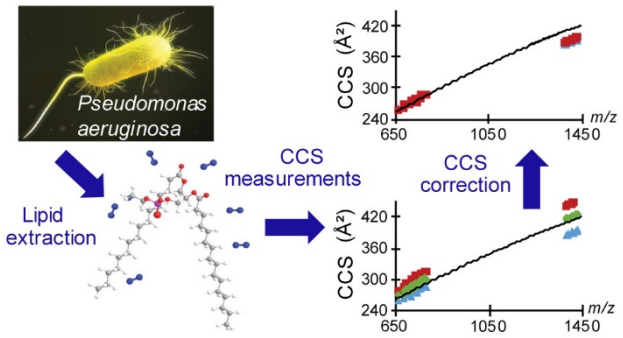

INTRODUCTION

Pseudomonas aeruginosa is a bacterium known to have intrinsic resistances to antibiotics and easily acquire genes encoding resistance to new drugs [1]. This bacterium is responsible of 18% of the bacteria-induced nosocomial pneumonia [2] which, combined with its virulence, dramatically increases the death rate of immunocompromised patients. As a result, *P. aeruginosa* is one of the deadliest bacteria in hospitals, thus ranked by the World Health Organization (WHO) as priority number one for the R&D of new antibiotics [3].

Due to the numerous resistance mechanisms of *P. aeruginosa* against antibiotics targeting proteins or enzymes [4], new antibiotic strategies are required. One of the current new drug strategies involves membrane cell destabilization or destruction leading to the bacteria lysis [5]. Thus, it is necessary to know the composition and 3D structure of the membrane cell lipids to develop such antibiotics. However, while the proteome of *P. aeruginosa* has been extensively studied [6–8], only few data have been reported on the mem- brane cell lipidome of *P. aeruginosa* [9, 10].

Here, we focused on the membrane lipids of *P. aeruginosa* and especially on the identification of the different compounds by ion mobility spectrometry coupled to mass spectrometry (IMS-MS). IMS is a post-ionization separation technique in which analyte ions travel through an inert gas (generally N_2 or He) in a cell under the influence of an electric field. For equal charge state, the most compact ions will have the smallest drift times since they are less slowed down by the buffer gas than the largest ions. Consequently, the IMS separation depends on charge, size and shape [11, 12]. Moreover, drift time (t_D) can be converted to the experimental collision cross section (CCS) of the ion within the buffer gas. CCS values are closely related to the 3D structure of each ion. These experimental CCS can be compared with calculated CCS obtained from theoretical structures using computational methods (*i.e.* trajectory meth- od (TM), projection approximation (PA) and exact hard sphere scattering (EHSS) methods [13]) or CCS predicted by using a machine learning approach [14] as CCS are predictable values [15].

For CCS determination, in most cases, and in particular for non-uniform field instruments such as traveling wave ion mobility spectrometry (TWIMS), the use of calibration is required with compounds of known CCS [16]. As an example, polyalanine, one of the most common calibrant for TWIMS, has been used for lipid CCS determination [17–19]. However, caution must be taken when choosing calibrants since shifts with the literature can be observed when using calibrants not chemically close to the sample [13]. Indeed, Hines *et al.* [20] confirmed that using calibrants structurally close to targets reduced the error in calibrated CCS values obtained with TWIMS. Thus, PCs are recommended for phospholipid calibration in positive mode and PEs for phospholipid calibration in negative mode [21]. Using definite calibrants, CCS values are extremely repeatable (RSD < 0.5%) [22], reproducible in intra-laboratory studies (RSD < 2%) [23] and reproducible in inter-laboratory studies (RSD < 5% using different ion mobility techniques, RSD < 2% using drift-tube) [19]. Consequently, CCS values can be used as an additional descriptor, together with *m/z* and retention time, to increase the confidence in automatic identification [19, 24]. For such reasons, the number of biological sample studies using IMS as a separation and characterization tool has been constantly increasing over the last decade [15, 17–20, 24–30].

Herein, we report the identification of the cell membrane phospholipids of *P. aeruginosa* strain PAK (PAK) and the experimental CCS values of their positive and negative ions. The data were acquired on a TWIMS, with nitrogen as drift gas, yielding $^{TW}CCS_{N2}$ values based on conventional notations [23]. To ensure our $^{TW}CCS_{N2}$ measurements, we used three approaches with different calibrating substances: (i) polyalanine [19] and (ii) lipid calibrants [20] which have been previously used for phospholipids, (iii) dextran which is a calibrant that can cover the required *m/z* and CCS ranges of PAK lipids, from the short fatty acyl chain phospholipids to the cardiolipins. We show here that the use of polyalanine or dextran requires a post-calibration $^{TW}CCS_{N2}$ correction using commercial phospholipid standards. This correction strategy was validated by comparing our corrected $^{TW}CCS_{N2}$ values with $^{DT}CCS_{N2}$ values of the literature. Then, the correction was applied to all the $^{TW}CCS_{N2}$ values of *P. aeruginosa* lipids. It is the first time to our knowledge that experimental $^{TW}CCS_{N2}$ values of both protonated and deprotonated ions of diphosphatidylglycerols—commonly called cardiolipins (CL)—are reported.

MATERIAL AND METHODS

Chemicals and reagents

Milli-Q grade water was obtained from an 18 MΩ Milli-Q (EMD Millipore Corporation, Molsheim, France). Methanol, chloroform, acetonitrile and isopropanol were purchased from Fischer Scientific (UK), ammonium formate from Sigma-Aldrich (Saint Quentin Fallavier, France) and formic acid from Merck (Germany). Except for chloroform which was HPLC grade, all solvents and buffers used were LC-MS grade. Polyalanine and dextran, used as IMS calibration substances, were purchased from Sigma-Aldrich (Saint Quentin Fallavier, France). Phospholipid standards for the IMS calibration were purchased from Avanti Polar Lipids (AL, USA): PE 6:0/6:0, PE 10:0/10:0, PE 15:0/15:0, PE 17:0/17:0, PC 17:0/17:0, PC 20:0/20:0, PC 24:0/24:0. Leucine enkephalin was purchased from Sigma-Aldrich (Saint Quentin Fallavier, France).

Biological sample preparation

A *P. aeruginosa* strain PAK (PAK) was pre-cultured in a 50-mL centrifugal tube containing 20 µL of bacterial stock solution (Muller-Hinton Broth (MHB)/glycerol, 70/30) and 20 mL of MHB. The flask was incubated overnight at 37 °C on a rotary shaker (140 rpm). After incubation, the pre-culture was used to inoculate 330 mL of MHB at a final concentration of 10^4 colony-forming units (CFU)/mL in a 1 L Erlenmeyer flask. The culture was incubated on a rotary shaker (140 rpm) at 37 °C for 7 h. Then, the culture was centrifuged (2600×*g*, 10 min, 20 °C). The obtained pellet was washed in 10 mL of 100 mM Tris pH 8.0. Ten milliliters of phosphate-buffered saline (PBS) and 3 mg of alginate lyase were added at room temperature during 1 h for the lysis of alginates, produced by *P. aeruginosa* PAK strain, which can be deleterious for mass spectrometric analysis. A pellet was obtained by centrifugation (5000×*g*, 10 min, 20 °C) and washed in 100 mM Tris pH 8.0. The pellet was resuspended in 6 mL of 100 mM Tris pH 8.0 and was subjected to sonication (cycles of 30 s on/10 s off for 2 min). The suspension was then centrifuged (5200×*g*, 20 min, 20 °C). The supernatant, containing the inner and outer membranes, was ultra-centrifuged (70,000×*g*, 1 h, 4 °C), then the resulting pellet was stocked at -20 °C.

Finally, the lipid extraction was carried out according to an adapted Bligh and Dyer protocol [31]. After waiting for the pellet to warm up to room temperature, 500 µL of Milli-Q water was added to dissolve the pellet and then vortex mixed for 5 min. 1.2 mL of methanol was added and then vortex mixed for 15 min. To degrade and eliminate proteolipids, the mixture was centrifuged (4000×*g*, 10 min, 22 °C), then the liquid phase was recovered. After adding 0.6 mL of chloroform, the solution was vortex mixed for 15 min and sonicated for 15 min. 0.6 mL of chloroform was added and then vortex mixed for another 15 min. 0.62 mL of a 1 M ammonium acetate was added and vortex mixed for 15 min. Finally, the mixture was left to rest for 30 min in order to allow the three phase separation (aqueous phase, protein interphase and organic phase). One milliliter of the organic phase was recovered and 0.94 mL of chloroform was added to the aqueous phase for a second liquid-liquid extraction. After stirring for 15 min, the mixture was left to rest again for 30 min. The aqueous phase was removed and organic phases were mixed and evaporated under argon. The organic phase was separated in aliquots and evaporated under argon. Lipid extracts were conserved under argon at -20 °C. To ascertain the quantity of lipids obtained, one aliquot of the lipid extract was diluted in a chloroform: methanol (4/1, v/v) solution. Then, the lipid extract concentration was checked by measuring the surface pressure of Langmuir monolayers.

Sample and calibrant mix solution preparation

The lipids extracted from the membrane of PAK were reconstituted in chloroform/methanol (2/1, v/v) to obtain a concentration of 1 µg/µL which was estimated as previously mentioned. Five microliters of this solution was then diluted in 20 µL of isopropanol/acetonitrile/water (4/3/1, v/v) for analysis. The dextran calibrant solution was prepared from a stock solution (1 mg/mL in water) diluted to 10^{-5} mol/L in water/ acetonitrile (1/1, v/v). The polyalanine calibrant solution was prepared from a stock solution (1 mg/mL in water/acetonitrile (1/1, v/v)) diluted to 10^{-5} mol/L in water/acetonitrile/acetic acid (49.5/49.5/1, v/v). Commercial PEs and PCs used as IMS standards were individually dissolved at 10^{-4} mol/L in chloroform/methanol (2/1, v/v), then mixed and diluted in isopropanol/acetonitrile/water (4/3/1, v/v) to obtain a lipid calibrant solution at 10^{-5} mol/L.

Instrumentation

The LC-IMS-MS experiments were performed using an UHPLC system (Dionex Ultimate 3000 RSLC, Thermo Scientific, San Jose, CA, USA) coupled to an IMS Q-TOF mass spectrometer (SYNAPT G2 HDMS, Waters MS Technologies, Manchester, UK) equipped with an electrospray interface, a traveling wave ion mobility (TWIMS) cell. Data treatment was performed with MassLynx 4.1, DriftScope 2.8 and UNIFI 1.8.2.169 software (Waters, Manchester, UK).

The column used was a 1.0 × 100 mm, Acquity UPLC CSH C18 1.7 µm column (Waters, Manchester, UK) equipped with a 0.2 µm prefilter. The sample tray and column oven temperatures were set at 4 °C and 50 °C, respectively. The injection volume was set at 1 µL. A flow rate of 100 µL/ min was used. Mobile phase A consisted of acetonitrile/ aqueous 10 mM ammonium formate (60/40) + 0.1 % formic acid and mobile phase B of isopropanol/acetonitrile/aqueous 10 mM ammonium formate (88/8/4) + 0.1 % formic acid. The gradient elution was the following: 0–3 min, 6–62% B; 3–8 min, 62–70% B; 8–13 min, 70% B; 13–15 min, 70–89% B; 15–20 min, 89% B; 20–22 min, 89–100% B; 22–26 min, 100% B; 26–27 min, 100–6% B; 27–30 min, 6% B.

LC-IMS-MS data were acquired in triplicate in positive and negative ion modes. The source parameters were in positive mode: capillary, extraction cone and cone voltages set at 3 kV, 6 V and 50 V, respectively; the cone gas and desolvation gas flows were 40 L/h and 600 L/h, respectively; and the desolvation temperature was 400 °C. For negative ion mode, the capillary, extraction cone and cone voltage were − 2.4 kV, 5 V and 45 V, respectively; the cone gas and desolvation gas flows were 60 L/h and 900 L/h, respectively; and the desolvation temperature was 500 °C.

The IMS parameters were helium cell flow 180 mL/min, traveling wave height 40 V, IMS cell nitrogen flow 70 mL/min (3.01 mbar) and traveling wave velocity 600 m/s.

Mass spectra were recorded over a *m/z* 50–2000 range in resolution mode (resolution 20 000 FWHM). External *m/z* calibration was performed with a sodium formate solution.

Lockmass correction was performed by infusing leucine enkephalin (2 ng/µL, 3 µL/min) via the LockSpray™ interface (reference scan frequency, lock spray capillary and cone voltage of 10 s, 3.5 kV and 40 V, respectively, in positive mode and 10 s, 2.5 kVand 30 V, respectively, in negative mode).

MS/MS experiments were performed in both positive and negative ionization mode. Precursor ions were selected in the quadrupole, at a resolution of 1 *m/z* unit, using retention time windows in the acquisition method. Several acquisitions were performed to obtain the MS/MS spectra for all co-eluting lipids. The collisional activation was performed in the trap cell using argon as target gas (6.10^{-3} mbar) and a collision energy of 35 eV. MS/MS spectra were processed using MassLynx 4.1 (Waters).

For calibrants, raw data were first opened with DriftScope 2.8 (Waters) in order to only select the singly charged ions on the 2D map (drift times plotted against *m/*z). Ion mobility spectra were then exported and processed with MassLynx 4.1 (Waters). For PAK samples, raw data were processed with UNIFI 1.8.2.169 (Waters). PAK lipids were first manually identified in order to create a home-made library from retention time (t_R) and *m/*z, for each of the lipids described in this publication. This library was then used to automatically obtain the lipids t_D.

Collision cross section measurements

Due to the use of an inhomogeneous electric field in the TWIMS cell, an external CCS calibration is required. For this purpose, we used singly charged ions of three published calibrants: dextran oligomers [32, 33], polyalanine oligomers [34] and phospholipids (PEs and PCs) [20]. Thus, these calibrant solutions were individually infused for 2 min in positive and negative modes. Ion mobility spectra were fitted with a Gauss function [35] using OriginPro 2016 9.3.226 (OriginLab Corporation) to obtain the drift time of each calibrant ion. Using charge- and mass-independent $^{DT}CCS_{N2}$ values (CCS') and drift times (t_D), calibration curves ln CCS' = f(ln t_D), for singly charged positive and negative ions, were obtained in nitrogen according to the procedure of Smith [16]. LC-IMS-MS data of the PAK sample were

processed with the UNIFI software (Waters) in order to automatically obtain drift time values.

Drift time values were collected for retention time variation lower than 0.3 min, mass error lower than 5 ppm and relative intensity higher than 0.1%.

Then, $^{TW}CCS_{N2}$ were determined using the calibration curve established previously. Finally, the $^{TW}CCS_{N2}$ values were corrected using the CCS correction strategy that will be developed in the results section of this paper. This correction involves plotting $^{DT}CCS_{N2}$ against $^{TW}CCS_{N2}$, for the phospholipid CCS standards, using calculation spreadsheets (see Electronic Supplementary Material (ESM) ESM_3).

RESULTS AND DISCUSSION

Lipid profiling

The LC-IMS-MS analysis of PAK membrane extract is reported in Fig. 1. The LC dimension allows the separation of the different classes of lipids, *i.e.* phosphatidylcholines (PC), phosphatidylethanolamines (PE), phosphatidylglycerols (PG) and cardiolipins (CL). Using our chromatographic conditions, the following separation could be achieved: PC, PE and PG classes (two fatty acid chains on phospholipids) from 8.5 to 12 min and CL class (four fatty acid chains on phospholipids) from 18.8 to 20.5 min. Some co-elution was still observed for isomers of phospholipids exhibiting different combinations of fatty acyl chains (*e.g.* PG 16:1/16:0 and PG 18:1_14:0, see ESM_1 Fig. S1) and for phospholipids consisted of fatty acyl chains showing two methylene and one more double bond (noted as DBE for double bond equivalent) than other phospholipids of the same class (*e.g.* PE 30:0, PE 32:1 and PE 34:2). Lipid identification was achieved thanks to the orthogonal MS dimension, more precisely from MS/MS data and accurate mass measurements.

Thus, 41 lipids were clearly identified in the membrane of PAK (see ESM_1: Tables S1, S2, and S3): 28 phospholipids (8 PGs, 13 PEs and 7 PCs) and 13 CLs. Please note that with our analytical conditions (*i.e.* buffered mobile phases), the cardiolipins were detected as singly

charged species but not as doubly charged species—as previously described with other analytical conditions [36]. The lipid annotation is based on the nomenclature of Liebisch *et al.* [37].

To our knowledge, this study is the first one on the membrane lipids of the strain PAK — other studies were performed on the strains PAO1 and PA14 [9, 10]. No relevant differences between the membrane lipids of the strains PAK, PAO1 and PA14 were observed.

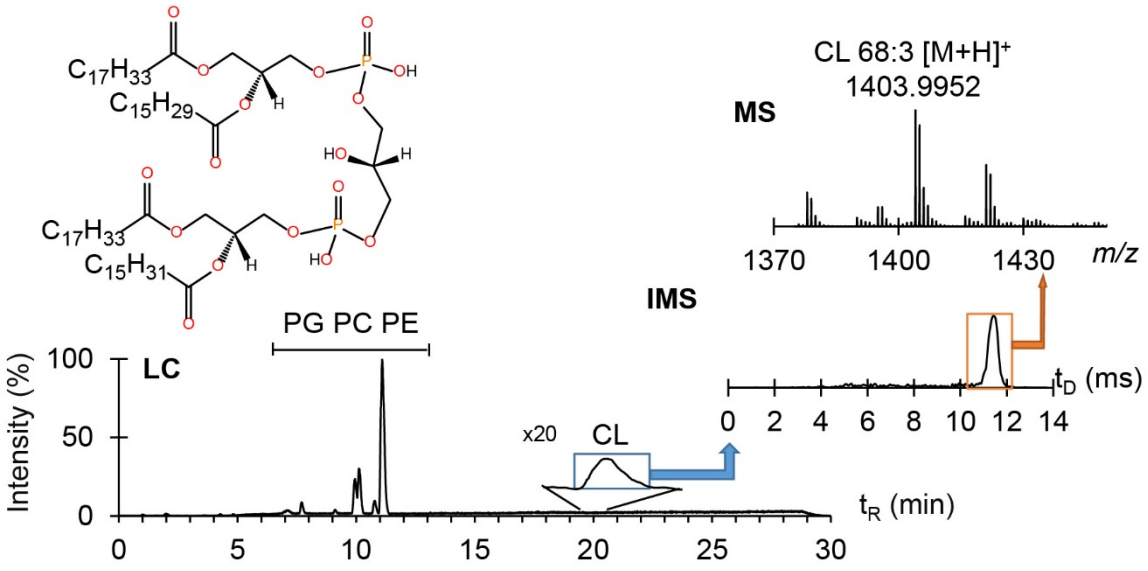

Fig. 1 Base Peak Chromatogram (BPC), extracted ion mobility spectrum and mass spectrum from LC-IMS-MS analysis of PAK membrane extract. The enlarged retention time zone corresponds to cardiolipins. The ion mobility spectrum was extracted for CL 68:3 (*m/z* 1403.9952). The mass spectrum is obtained by integrating the ion mobility spectra from 10.5 ms to 12.5 ms. A possible structure for *m/z* 1403.9952 is given on the left.

$^{TW}CCS_{N2}$ determination, comparison with published CCS values and post-calibration correction

Most of the CCS reported in the literature for phospholipids (PL) have been obtained using either a drift-tube IMS instrument [15, 20, 38, 39] or a TWIMS cell calibrated with polyalanine ions [17–19]. In the latter case, Hines *et al.* [20, 25] had previously

demonstrated that the $^{TW}CCS_{N2}$ determination of PL requires TWIMS cell calibration with PL calibrants. However, obtaining the most representative $^{TW}CCS_{N2}$ values would require to have lipid calibration curves for each chemical class present in the sample (PC, PE, PG or CL) and for each number of double bonds on the fatty acyl chains (0, 1 or 2).

Because of the lack of such calibrants, we chose to use a single calibrant to determine the CCS values of all the PAK membrane lipids. For this reason, we choose the dextran calibrant which covers the required *m/z* and CCS ranges, in particular for CLs.

Please note that an extrapolated polyalanine calibration was considered as well, but for clarity, the following methodology will be described for the dextran calibration first. The calibration curves obtained with dextran (in both positive and negative modes) were then used for our PAK sample (see ESM_2). Thus, the $^{TW}CCS_{N2}$ of $[M+H]^+$ were measured for PEs, PCs and CLs in positive ion mode while the $^{TW}CCS_{N2}$ of $[M-H]^-$ were measured for PEs, PGs and CLs in negative ion mode. Triplicate of $^{TW}CCS_{N2}$ measurements were carried out for each sample (in positive and negative ion mode) and gave repeatable CCS values ($0.1\% \leq \%RSD \leq 0.4\%$, $n = 3$). However, when we compared our measured $^{TW}CCS_{N2}$ values with those published (5 PEs and 6 PCs inpositive mode, 6 PEs and 4 PGs in negative mode), shifts in CCS were systematically observed ($\Delta CCS \geq 2\%$) (ESM_1: Tables S4 and S5). This is also illustrated in Fig. 2a: the ex- perimental $^{TW}CCS_{N2}$ values obtained after dextran calibration in positive ion mode (red squares) are significantly shifted towards higher CCS values compared with the lipid CCS values from the literature [20] (extrapolated black line).

In order to avoid this issue, we propose here a CCS correction strategy to reduce the shift due to the dextran calibration. The CCS correction strategy was carried out, using the IMS lipid calibrants (PEs and PCs, see ESM_2), by plotting correlation curves between their experimental $^{TW}CCS_{N2}$ calibrated with dextran and their published $^{DT}CCS_{N2}$ [20]. In both positive and negative ion mode, a linear regression was obtained with high coefficient of determination ($R2 \geq 0.999$, ESM_3). This post-calibration correction was then applied to the $^{TW}CCS_{N2}$ values of lipids present in PAK strain (red squares of Fig. 2b). Please note that previous work had shown that the fatty acyl chains of phospholipids extracted from *P. aeruginosa* can be different from the ones of eukaryotes —especially odd-chains which can

be cyclopropylated or methylated [9, 40]. However, considering the resolving power of TWIMS, linear, cyclopropylated or methylated fatty acyl chain isomers would not be separated. Hence, we could use easily available phospholipid standards rather than bacterial phospholipids for the correction.

In parallel, as proof of concept for our correction strategy, we also determined $^{TW}CCS_{N2}$ for PAK lipids using polyalanine or lipid calibration curves (see ESM_2). These calibration curves were extrapolated to higher CCS values in order to exceed those of CLs.

The experimental $^{TW}CCS_{N2}$ for PAK lipids, using these extrapolated calibration curves, are reported in Fig. 2a as green (polyalanine cal) and blue (PL cal) points. One can notice that the CCS range of our $^{TW}CCS_{N2}$ obtained with polyalanine calibration (ESM_1: Table S2) are consistent with the cardiolipins $^{TW}CCS_{N2}$ of $[M+2K]^{2+}$ and $[M-2H]^{2-}$ from *Escherichia coli* recently published by Hines *et al.* (CCS range of 380−425 $Å^2$) [25]. The correction strategy, previously described for the $^{TW}CCS_{N2}$ calibrated with dextran, was also applied for $^{TW}CCS_{N2}$ values calibrated with polyalanine (green points of Fig. 2b).

Figure 2b shows that the correction strategy applied for $^{TW}CCS_{N2}$ values calibrated by either dextran or polyalanine, and the $^{TW}CCS_{N2}$ calibration —without correction— with PL, lead to convergent experimental $^{TW}CCS_{N2}$ values. Moreover, for CLs, these convergent $^{TW}CCS_{N2}$ values are smaller than the extrapolated PE/PC $^{DT}CCS_{N2}$ black line. This result suggests that cardiolipins are more compact (smaller $^{TW}CCS_{N2}$ value) than any PE or PC which would have a similar m/z value (extrapolated black line). This might be explained by the fact that cardiolipins are biosynthesized from a phosphatidylglycerol and a phosphatidic acid [41] which have smaller CCS values than PEs or PCs [15]. The details of all the $^{TW}CCS_{N2}$ values we measured are reported in the supplementary information (ESM_1: Tables S1 to S3): $^{TW}CCS_{N2}$ values using the three types of calibration (dextran (Table S1), polyalanine (Table S2) and lipids (Table S3)) and the two corrections (dextran corrected with lipids (Table S1) and polyalanine corrected with lipids (Table S2).

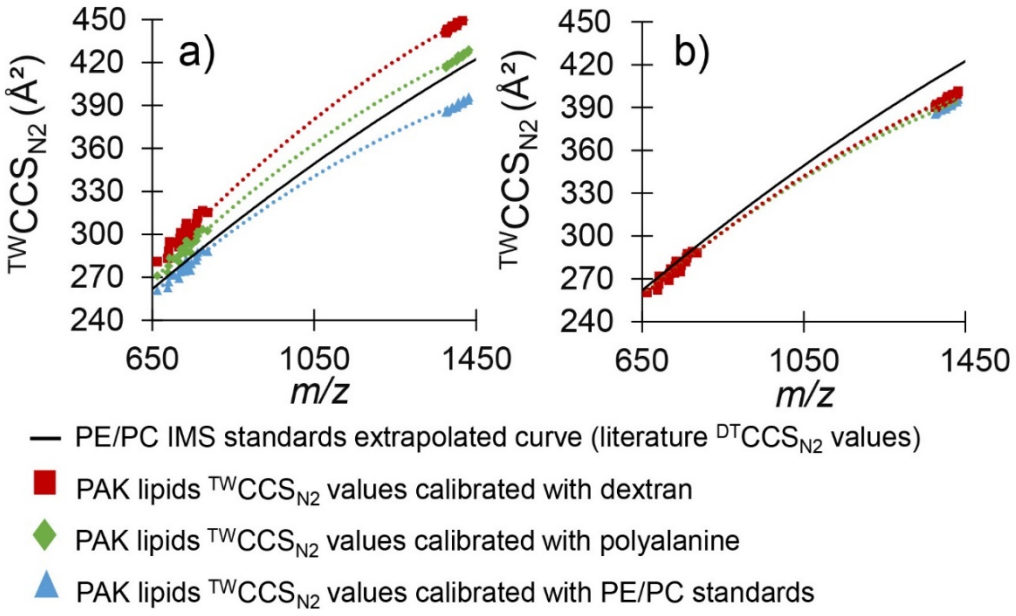

Fig. 2 $^{TW}CCS_{N2}$ plotted against *m/z* for positive ions of PAK lipids. (a) represents $^{TW}CCS_{N2}$ of PAK lipids before correction of the $^{TW}CCS_{N2}$ values. (b) represents $^{TW}CCS_{N2}$ of PAK lipids after the correction. In both (a) and (b), the black line represents the lipid IMS standards extrapolated curve ($^{DT}CCS_{N2}$ values from Hines *et al.* [20]). $^{TW}CCS_{N2}$ of PAK lipids are represented by red squares when calibrated with dextran, green squares when calibrated with polyalanine and blue squares when calibrated with lipid standards.

In order to validate our correction strategy (calibration with dextran followed by a post-calibration correction with lipids, as mentioned above), the corrected $^{TW}CCS_{N2}$ values were compared with the published ones. Note that several phospholipids (PEs, PGs and PCs) present in our sample had published CCS values (17 in positive mode and 16 in negative mode). On the other hand, CCS values of protonated and deprotonated prokaryote cardiolipins had never been reported. Considering that published CCS values from different ion mobility techniques have some disparities (0.04% ≤ ΔCCS% ≤ 3.84 %, ESM_1: Tables S6 and S7), our $^{TW}CCS_{N2}$ are consistent with the CCS values from the literature, as reported in Table S5. One can note that the CCS disparities in the literature could be due to differences in lipid structures (*e.g.* double bond location and geometry cis/trans). This structural heterogeneity would give rise to small, but measurable, CCS difference [38].

In addition, one can observe that the correction strategy allows a shift reduction to less than 2% between our corrected $^{TW}CCS_{N2}$ and those reported by Zhou *et al.* [15] and Hines *et al.* [20], as shown in Table 1. Since such deviation is acceptable for inter-laboratory reproducibility, we can highlight the validation of the post-calibration correction strategy. Furthermore, the $^{TW}CCS_{N2}$ values of phospholipids extracted from PAK membrane are similar to the CCS values of lipid standards from the literature; therefore, we can suppose that the phospholipids in PAK have similar tridimensional structures in gas phase than the phospholipids used by Zhou *et al.* and Hines *et al.* (synthetic standards) [15, 20]. Besides, a similar decrease of the shift between our experimental $^{TW}CCS_{N2}$ values and those of the literature was observed for the experimental CCS values obtained by polyalanine calibration and post-calibration lipid correction, as illustrated in Fig. 2b. All comparisons with the literature are given in ESM_1 Tables S4 and S5.

Table 1. Comparison of our experimental $^{TW}CCS_{N2}$, from PAK, with the published values. a and b correspond to relative shifts between our CCS and $^{DT}CCS_{N2}$ from a: Zhou *et al.* (2017) [15] and b: Hines *et al.* (2016) [20], respectively.

Positive ion mode $[M+H]^+$						
Lipid	Calibration using dextran			After calibration correction		
	$^{TW}CCS_{N2}$ (Å^2)	ΔCCS^a (%)	ΔCCS^b (%)	$^{TW}CCS_{N2}$ (Å^2)	ΔCCS^a (%)	ΔCCS^b (%)
PC 32:0	307.6	8.0	8.9	282.0	-1.0	-0.2
PE 32:0	294.6	7.8	8.5	271.4	-0.7	0.0
PE 34:0	301.0	7.5	8.5	276.6	-1.2	-0.3
PE 34:1	297.1	7.4	8.7	273.4	-1.2	0.0

Negative ion mode $[M-H]^-$						
Lipid	Calibration using dextran			After calibration correction		
	$^{TW}CCS_{N2}$ (Å^2)	ΔCCS^a (%)	ΔCCS^b (%)	$^{TW}CCS_{N2}$ (Å^2)	ΔCCS^a (%)	ΔCCS^b (%)
PE 32:0	274.4	5.6	5.8	257.1	-1.1	-0.9
PE 34:0	281.4	5.7	6.0	263.4	-1.1	-0.8
PE 34:1	279.5	5.5	5.7	261.6	-1.3	-1.1

CCS correction application

Once the post-calibration correction was validated, this methodology was then extended to all the lipids of PAK. Table 2 reports the $^{TW}CCS_{N2}$ values of lipids in PAK extracts which constitute new findings, in particular for CLs. Indeed, the $^{TW}CCS_{N2}$ of $[M+H]^+$ and $[M-H]^-$ are determined for the first time for PAK cardiolipins (Table 2, ESM_1: Tables S1 to S3). As previously mentioned, the doubly charged cardiolipins were not detected since the ionization of the singly charged species was favored by our analytical conditions. In the case of phospholipids, we could verify that our corrected experimental CCS were consistent with those of phospholipids de- scribed in literature (ESM_1: Tables S4 and S5).

In total, 56 $^{TW}CCS_{N2}$ values were measured and corrected, including 32 for positive ions and 24 for negative ions. Using the dextran calibration, the $^{TW}CCS_{N2}$ range was from 303 Å² to 455 Å² in positive mode and from 266 Å² to 418 Å² in negative mode, whereas when the dextran calibration was corrected, the $^{TW}CCS_{N2}$ range was from 278 Å² to 401 Å² in positive mode and from 249 Å² to 387 Å² in negative mode. More precisely for cardiolipins, the $^{TW}CCS_{N2}$ range was from 441 Å² to 455 Å² in positive mode and from 411 Å² to 418 Å² in negative mode, whereas when the dextran calibration was corrected, the $^{TW}CCS_{N2}$ range was from 390 Å² to 401 Å² in positive mode and from 380 Å² to 387 Å² in negative mode. Moreover, for cardiolipins in negative mode, the $^{TW}CCS_{N2}$ values were consistent with the first two $^{DT}CCS_{N2}$ of CL (CL 72:6 and CL 72:7) described from bovine heart by Groessl *et al.* [38].

Table 2. $^{TW}CCS_{N2}$ values, with dextran calibration and lipid correction, for phospholipids extracted from the membrane of PAK.

Origin	Lipid	$^{TW}CCS_{N2}$ (Å²) for $[M+H]^+$	$^{TW}CCS_{N2}$ (Å²) for $[M-H]^-$
Phospholipids extracted from the membrane of PAK	PE 30:1	260.2	249.7
	PE 33:1	271.0	258.7
	PE 35:1	276.0*	264.9
	PG 30:0	nd	258.3
	PG 35:2	nd	269.7
	CL 66:3	390.1	380.4
	CL 66:2	391.2	381.6
	CL 66:1	391.9	nd
	CL 67:3	392.8	nd
	CL 67:2	393.7	nd
	CL 68:4	394.0	nd
	CL 68:3	395.7	nd
	CL 68:2	397.4	386.9
	CL 69:4	396.7	nd
	CL 69:3	398.3	nd
	CL 69:2	399.0	nd
	CL 70:4	399.4	nd
	CL 70:3	401.2	nd

These values are new to the literature, apart from the CCS noted with *. nd: not detected.

PAK lipid $^{TW}CCS_{N2}$ vs m/z correlation

Fig. 3 illustrates the correlation between the corrected $^{TW}CCS_{N2}$ values and *m/z* values in negative mode: for all lipids in Fig. 3a and for PEs and PGs in Fig. 3b. As shown in Fig. 3a, a polynomial fit for $^{TW}CCS_{N2}$ plotted against *m/z* in negative mode (> 0.999) was observed. A polynomial fit (> 0.99) was also observed for positive values (ESM_1: Fig. S9). By plotting $^{TW}CCS_{N2}$ against *m/z* for each chemical family, we can observe that PGs, PEs and CLs present similar slopes.

In negative ion mode, deprotonated molecules of PEs and PGs present close $^{TW}CCS_{N2}$ values for a same *m/z* range (Fig. 3b), also for PEs and PGs constituted of the same acyl chains. The

$^{TW}CCS_{N2}$ of PGs are slightly higher than the ones of the PEs (*e.g.* $^{TW}CCS_{N2}$(PG 34:1) = 268.5 Å² > $^{TW}CCS_{N2}$ (PE 34:1) = 261.6 Å²). A similar trend was observed for PEs and PCs, in positive mode, with PC's $^{TW}CCS_{N2}$ being slightly higher than the ones of the PEs (ESM_1: Fig. S9).

Moreover, as shown in Fig. 3b, we can make several observations. First, as previously described by Jackson *et al.* [28], the CCS linearly decreases when the number of double-bonds increases in the fatty acyl chains for definite chain lengths (*e.g.* C32:0, C32:1 and C32:2). Secondly, the slope observed from this linear pattern was identical for every chemical classes, leading to a symmetrical figure, as described by Leaptrot *et al* [39]. Thirdly, for positive ions (ESM_1: Fig. S9), CCS values of phospholipids with odd number of carbon atoms in the fatty acyl chains and with 0, 1 or 2 DBE were closer than the CCS values of phospholipids with even number of carbon atoms. All of these observations could be explained by the folding of the fatty acyl chain with the increase of the DBE, as previously described [15,28,42].

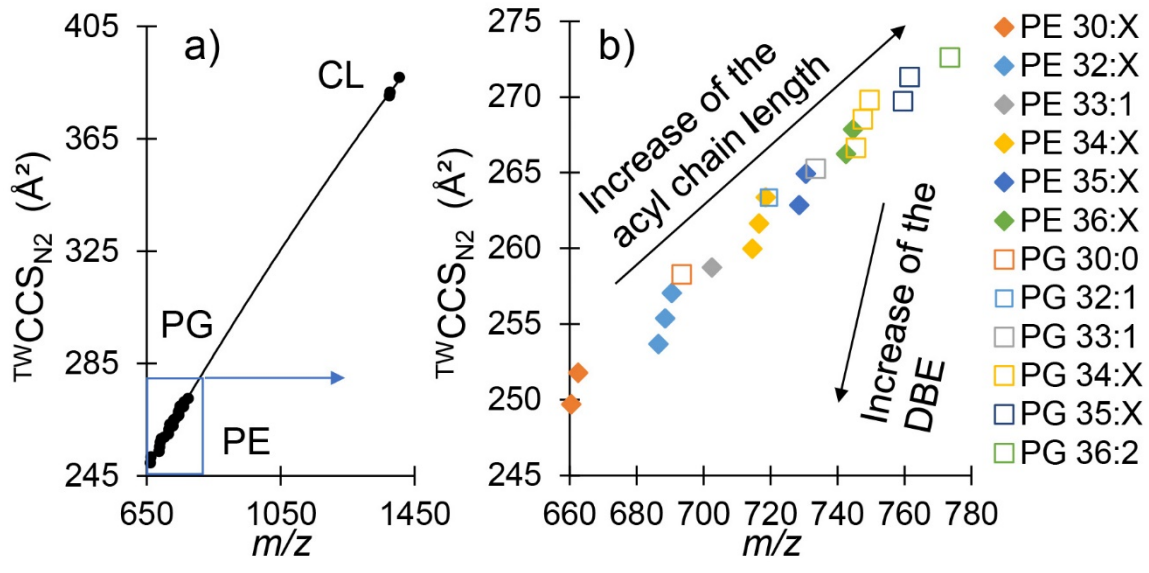

Fig. 3 $^{TW}CCS_{N2}$ values plotted against *m/z* for negative ions. 3a represents values for every class of phospholipids, whereas 3b only represents values for PEs and PGs. 3b was inspired from the Fig. 4 from Zhou et al (2017) [15]. PGs are represented by squares, PEs by diamonds. X refers to the number of double-bonds on the fatty acid moiety of the phospholipid which can be 0, 1 or 2 for PEs and PGs.

CONCLUSION

In this study, new knowledge about the membrane phospholipids of *P. aeruginosa* was obtained. In particular, new prokaryote lipid CCS values were determined. We worked on a methodology to allow the measurement of $^{TW}CCS_{N2}$ within high *m/*z and CCS ranges. Our work resulted in a CCS correction strategy. After applying the correction, we showed that the CCS deviation observed between the CCS values of the literature and the ones measured with the dextran or polyalanine calibration could be lessened. We measured 32 $^{TW}CCS_{N2}$ values in positive ionization mode and 24 in negative mode, with a good repeatability (RSD ≤ 0.4%). In particular, we measured 18 new $^{TW}CCS_{N2}$ values for cardiolipins, a unique class of phospholipids whose CCS values were lacking in the literature for protonated and deprotonated molecules. Such values can be used to complete existing CCS databases. Moreover, regarding antibiotic research against *P. aeruginosa*, cardiolipins are of high interest as a recent study described new antibiotic therapies targeting cardiolipins [43].

FUNDING INFORMATION

The authors gratefully acknowledge European Regional Development Fund (ERDF, no. HN0001343), Labex SynOrg (ANR-11-LABX-0029) and Région Normandie for their financial support.

COMPLIANCE WITH ETHICAL STANDARDS

CONFLICT OF INTEREST

The authors declare that they have no conflict of interest.

REFERENCES

1. Obritsch MD, Fish DN, MacLaren R, Jung R (2005) Nosocomial Infections Due to Multidrug-Resistant *Pseudomonas aeruginosa*: Epidemiology and Treatment Options. PHARMACOTHERAPY 25 (10):11

2. Curran CS, Bolig T, Torabi-Parizi P (2018) Mechanisms and Targeted Therapies for *Pseudomonas aeruginosa* Lung Infection. American journal of respiratory and critical care medicine 197 (6):708-727. doi:10.1164/rccm.201705-1043SO

3. Tacconelli E, *et al.* (2018) Discovery, research, and development of new antibiotics: the WHO priority list of antibiotic-resistant bacteria and tuberculosis. The Lancet Infectious Diseases 18 (3):318-327. doi:10.1016/s1473-3099(17)30753-3

4. Bassetti M, Vena A, Croxatto A, Righi E, Guery B (2018) How to manage *Pseudomonas aeruginosa* infections. Drugs Context 7:212527. doi:10.7573/dic.212527

5. Escriba PV (2006) Membrane-lipid therapy: a new approach in molecular medicine. Trends Mol Med 12 (1):34-43. doi:10.1016/j.molmed.2005.11.004

6. Gaviard C, Jouenne T, Hardouin J (2018) Proteomics of *Pseudomonas aeruginosa*: the increasing role of post-translational modifications. Expert Rev Proteomics 15 (9):757-772. doi:10.1080/14789450.2018.1516550

7. Kamath KS, Krisp C, Chick J, Pascovici D, Gygi SP, Molloy MP (2017) *Pseudomonas aeruginosa* Proteome under Hypoxic Stress Conditions Mimicking the Cystic Fibrosis Lung. Journal of proteome research 16 (10):3917-3928. doi:10.1021/acs.jproteome.7b00561

8. Hare NJ, Solis N, Harmer C, Marzook NB, Rose B, Harbour C, Crossett B, Manos J, Cordwell SJ (2012) Proteomic profiling of *Pseudomonas aeruginosa* AES-1R, PAO1 and PA14 reveals potential virulence determinants associated with a transmissible cystic fibrosis-associated strain. BMC Microbiol 12:16. doi:10.1186/1471-2180-12-16

9. Benamara H, Rihouey C, Abbes I, Mlouka MAB, Hardouin J, Jouenne T, Alexandre S (2014) Characterization of Membrane Lipidome Changes in *Pseudomonas aeruginosa* during Biofilm Growth on Glass Wool. Plos One 9 (9):9. doi:10.1371/journal.pone.0108478.g001

10. Benamara H, Rihouey C, Jouenne T, Alexandre S (2011) Impact of the biofilm mode of growth on the inner membrane phospholipid composition and lipid domains in *Pseudomonas aeruginosa*. Biochim Biophys Acta 1808 (1):98-105. doi:10.1016/j.bbamem.2010.09.004

11. Ewing MA, Glover MS, Clemmer DE (2016) Hybrid ion mobility and mass spectrometry as a separation tool. J Chromatogr A 1439:3-25. doi:10.1016/j.chroma.2015.10.080

12. Cumeras R, Figueras E, Davis CE, Baumbach JI, Gracia I (2015) Review on ion mobility spectrometry. Part 1: current instrumentation. Analyst 140 (5):1376-1390. doi:10.1039/c4an01100g

13. Gabelica V, Marklund E (2018) Fundamentals of ion mobility spectrometry. Curr Opin Chem Biol 42:51-59. doi:10.1016/j.cbpa.2017.10.022

14. Plante PL, Francovic-Fontaine E, May JC, McLean JA, Baker ES, Laviolette F, Marchand M, Corbeil J (2019) Predicting Ion Mobility Collision Cross-Sections Using a Deep Neural Network: DeepCCS. Anal Chem 91 (8):5191-5199. doi:10.1021/acs.analchem.8b05821

15. Zhou Z, Tu J, Xiong X, Shen X, Zhu ZJ (2017) LipidCCS: Prediction of Collision Cross-Section Values for Lipids with High Precision To Support Ion Mobility-Mass Spectrometry-Based Lipidomics. Analytical chemistry 89 (17):9559-9566. doi:10.1021/acs.analchem.7b02625

16. Smith DP, Knapman TW, Campuzano I, Malham RW, Berryman JT, Radford SE, Ashcroft AE (2009) Deciphering drift time measurements from travelling wave ion mobility spectrometry-mass spectrometry studies. European journal of mass spectrometry 15 (2):113-130. doi:10.1255/ejms.947

17. Paglia G, Astarita G (2017) Metabolomics and lipidomics using traveling-wave ion mobility-mass spectrometry. Nat Protoc 12 (4):17. doi:10.1038/nprot.2017.013

18. Paglia G, Kliman M, Claude E, Geromanos S, Astarita G (2015) Applications of ion-mobility mass spectrometry for lipid analysis. Anal Bioanal Chem 407:12

19. Paglia G, Williams JP, Menikarachchi L, Thompson JW, Tyldesley-Worster R, Halldorsson S, Rolfsson O, Moseley A, Grant D, Langridge J, Palsson BO, Astarita G (2014) Ion mobility derived collision cross sections to support metabolomics applications. Analytical chemistry 86 (8):3985-3993. doi:10.1021/ac500405x

20. Hines KM, May JC, McLean JA, Xu L (2016) Evaluation of Collision Cross Section Calibrants for Structural Analysis of Lipids by Traveling Wave Ion Mobility-Mass Spectrometry. Analytical chemistry 88 (14):7329-7336. doi:10.1021/acs.analchem.6b01728

21. Levy AJ, Oranzi NR, Ahmadireskety A, Kemperman RHJ, Wei MS, Yost RA (2019) Recent progress in metabolomics using ion mobility-mass spectrometry. TrAC Trends in Analytical Chemistry 116:274-281. doi:10.1016/j.trac.2019.05.001

22. Tejada-Casado C, Hernandez-Mesa M, Monteau F, Lara FJ, Olmo-Iruela MD, Garcia-Campana AM, Le Bizec B, Dervilly-Pinel G (2018) Collision cross section (CCS) as a complementary parameter to characterize human and veterinary drugs. Anal Chim Acta 1043:52-63. doi:10.1016/j.aca.2018.09.065

23. May JC, Morris CB, McLean JA (2017) Ion Mobility Collision Cross Section Compendium. Analytical chemistry 89 (2):1032-1044. doi:10.1021/acs.analchem.6b04905

24. Schrimpe-Rutledge AC, Sherrod SD, McLean JA (2018) Improving the discovery of secondary metabolite natural products using ion mobility-mass spectrometry. Curr Opin Chem Biol 42:160-166. doi:10.1016/j.cbpa.2017.12.004

25. Hines KM, Xu L (2019) Lipidomic consequences of phospholipid synthesis defects in Escherichia coli revealed by HILIC-ion mobility-mass spectrometry. Chemistry and physics of lipids 219:15-22. doi:10.1016/j.chemphyslip.2019.01.007

26. Zheng X, Aly NA, Zhou Y, Dupuis KT, Bilbao A, Paurus VL, Orton DJ, Wilson R, Payne SH, Smith RD, Baker ES (2017) A structural examination and collision cross section database for over 500 metabolites and xenobiotics using drift tube ion mobility spectrometry. Chem Sci 8 (11):7724-7736. doi:10.1039/c7sc03464d

27. Ridenour WB, Kliman M, McLean JA, Caprioli RM (2010) Structural characterization of phospholipids and peptides directly from tissue sections by MALDI traveling-wave ion mobility-mass spectrometry. Analytical chemistry 82 (5):1881-1889. doi:10.1021/ac9026115

28. Jackson SN, Ugarov M, Post JD, Egan T, Langlais D, Schultz JA, Woods AS (2008) A study of phospholipids by ion mobility TOFMS. Journal of the American Society for Mass Spectrometry 19 (11):1655-1662. doi:10.1016/j.jasms.2008.07.005

29. Harris RA, Leaptrot KL, May JC, McLean JA (2019) New frontiers in lipidomics analyses using structurally selective ion mobility-mass spectrometry. TrAC-Trend Anal Chem 116:316-323. doi:10.1016/j.trac.2019.03.031

30. Hinz C, Liggi S, Griffin JL (2018) The potential of Ion Mobility Mass Spectrometry for high-throughput and high-resolution lipidomics. Curr Opin Chem Biol 42:42-50. doi:10.1016/j.cbpa.2017.10.018

31. Bligh EG, Dyer WJ (1959) A rapid method of total lipid extraction and purification. Can J Biochem Physiol 37 (8):7

32. Hofmann J, Struwe WB, Scarff CA, Scrivens JH, Harvey DJ, Pagel K (2014) Estimating collision cross sections of negatively charged N-glycans using traveling wave ion mobility-mass spectrometry. Analytical chemistry 86 (21):10789-10795. doi:10.1021/ac5028353

33. Pagel K, Harvey DJ (2013) Ion mobility-mass spectrometry of complex carbohydrates: collision cross sections of sodiated N-linked glycans. Analytical chemistry 85 (10):5138-5145. doi:10.1021/ac400403d

34. Bush MF, Campuzano ID, Robinson CV (2012) Ion mobility mass spectrometry of peptide ions: effects of drift gas and calibration strategies. Analytical chemistry 84 (16):7124-7130. doi:10.1021/ac3014498

35. Domalain V, Hubert-Roux M, Tognetti V, Joubert L, Lange CM, Rouden J, Afonso C (2014) Enantiomeric differentiation of aromatic amino acids using traveling wave ion mobility-mass spectrometry. Chem Sci 5 (8):3234-3239. doi:10.1039/c4sc00443d

36. Garrett TA, Kordestani R, Raetz CRH (2007) Quantification of Cardiolipin by Liquid Chromatography-Electrospray Ionization Mass Spectrometry. 433:213-230. doi:10.1016/s0076-6879(07)33012-7

37. Liebisch G, Vizcaino JA, Kofeler H, Trotzmuller M, Griffiths WJ, Schmitz G, Spener F, Wakelam MJ (2013) Shorthand notation for lipid structures derived from mass spectrometry. Journal of lipid research 54 (6):1523-1530. doi:10.1194/jlr.M033506

38. Groessl M, Graf S, Knochenmuss R (2015) High resolution ion mobility-mass spectrometry for separation and identification of isomeric lipids. Analyst 140 (20):6904-6911. doi:10.1039/c5an00838g

39. Leaptrot KL, May JC, Dodds JN, McLean JA (2019) Ion mobility conformational lipid atlas for high confidence lipidomics. Nature communications 10 (1):985. doi:10.1038/s41467-019-08897-5

40. Chao J, Wolfaardt GM, Arts MT (2010) Characterization of *Pseudomonas aeruginosa* fatty acid profiles in biofilms and batch planktonic cultures. Can J Microbiol 56 (12):1028-1039. doi:10.1139/W10-093

41. Schlame M (2008) Cardiolipin synthesis for the assembly of bacterial and mitochondrial membranes. Journal of lipid research 49 (8):1607-1620. doi:10.1194/jlr.R700018-JLR200

42. Kim HI, Kim H, Pang ES, Ryu EK, Beegle LW, Loo JA, Goddard WA, Kanik I (2009) Structural characterization of unsaturated phosphatidylcholines using traveling wave ion mobility spectrometry. Analytical chemistry 81 (20):8289-8297. doi:10.1021/ac900672a

43. El Khoury M, Swain J, Sautrey G, Zimmermann L, Van Der Smissen P, Décout J-L, Mingeot-Leclercq M-P (2017) Targeting Bacterial Cardiolipin Enriched Microdomains: An Antimicrobial Strategy Used by Amphiphilic Aminoglycoside Antibiotics. Sci Rep 7 (1). doi:10.1038/s41598-017-10543-3

Supplementary Information S1 : MS/MS spectrum and $^{TW}CCS_{N2}$ measurements.

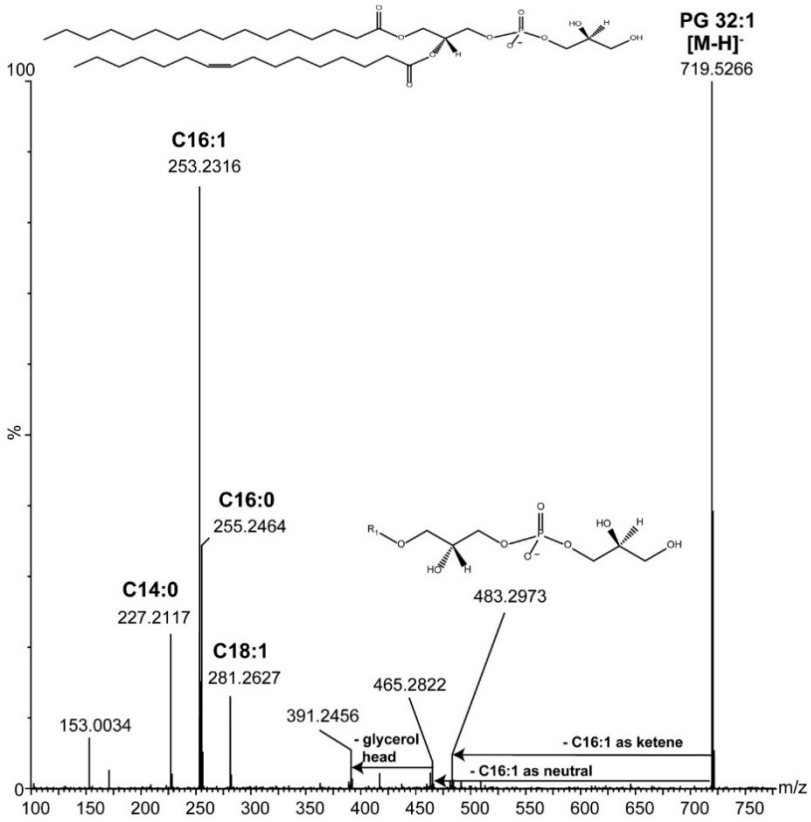

Fig S1. MS/MS Spectra of PG 32:1. A possible structure of the most abundant isomer is given (cis or trans isomerism cannot be determined with this experiment). The ion of *m/z* 153.0034 corresponds to the Glycerol-3-phosphate ion with loss of H_2O. The $[M-H]^-$ of the fatty acyl chains show the presence the isomers PG 16:0_16:1 and PG 14:0_18:1. Knowing that the loss of *sn-2* is favoured, since ions of *m/z* 483.2973, 465.2822, 391.2456 and 253.2316 are the most abundant, we can conclude that for PG 16:0/16:1, the most abundant isomer, the 16:0 is on position *sn-1* and the 16:1 is on position *sn-2*.

Structural elucidation was performed according to Hsu F-F, Turk J (2009) Electrospray Ionization with Low-energy Collisionally Activated Dissociation Tandem Mass Spectrometry of Glycerophospholipids: Mechanisms of Fragmentation and Structural Characterization. J Chromatogr B Analyt Technol Biomed Life Sci 877 (26):22.

89

Table S2 $^{TW}CCS_{N2}$ values calibrated with **dextran** for the membrane lipids of PAK

		Positive ions					Negative ions				
membrane lipids of PAK	**Formula**	**ion**	***m/z***	**$^{TW}CCS_{N2}$ without correction**	**$^{TW}CCS_{N2}$ %RSD**	**corrected $^{TW}CCS_{N2}$ (Å²)**	**ion**	***m/z***	**$^{TW}CCS_{N2}$ without correction**	**$^{TW}CCS_{N2}$ %RSD**	**corrected $^{TW}CCS_{N2}$ (Å²)**
PC 32:1	$C_{40}H_{78}NO_8P$	$[M+H]^+$	732.553	303.6	0.1	278.7					
PC 32:0	$C_{40}H_{80}NO_8P$	$[M+H]^+$	734.569	307.6	0.1	282.0					
PC 34:2	$C_{42}H_{82}NO_8P$	$[M+H]^+$	758.569	307.5	0.1	281.9					
PC 34:1	$C_{42}H_{82}NO_8P$	$[M+H]^+$	760.585	311.0	0.1	284.7					
PC 34:0	$C_{42}H_{84}NO_8P$	$[M+H]^+$	762.600	314.2	0.4	287.3					
PC 35:1	$C_{43}H_{84}NO_8P$	[M+H]+	774.600	316.3	0.1	289.0					
PC 36:2	$C_{42}H_{82}NO_8P$	$[M+H]^+$	786.600	315.1	0.1	288.1					
PE 30:1	$C_{35}H_{68}NO_8P$	$[M+H]^+$	662.475	280.8	0.1	260.2	$[M-H]^-$	660.461	266.3	0.1	249.7
PE 30:0	$C_{35}H_{70}NO_8P$						$[M-H]^-$	662.476	268.6	0.1	251.8
PE 32:2	$C_{37}H_{70}NO_8P$	$[M+H]^+$	688.491	283.2	0.1	262.2	$[M-H]^-$	686.476	270.7	0.2	253.7
PE 32:1	$C_{37}H_{72}NO_8P$	$[M+H]^+$	690.506	288.3	0.1	266.3	$[M-H]^-$	688.492	272.6	0.1	255.4
PE 32:0	$C_{37}H_{74}NO_8P$	$[M+H]^+$	692.522	294.6	0.0	271.4	$[M-H]^-$	690.507	274.4	0.1	257.1
PE 33:1	$C_{38}H_{74}NO_8P$	$[M+H]^+$	704.522	294.1	0.1	271.0	$[M-H]^-$	702.507	276.3	0.1	258.7
PE 34:2	$C_{39}H_{73}NO_8P$	$[M+H]^+$	716.522	291.4	0.1	268.8	$[M-H]^-$	714.507	277.7	0.1	260.0
PE 34:1	$C_{37}H_{76}NO_8P$	$[M+H]^+$	718.538	297.1	0.1	273.4	$[M-H]^-$	716.523	279.5	0.0	261.6
PE 34:0	$C_{39}H_{78}NO_8P$	$[M+H]^+$	720.553	301.0	0.1	276.6	$[M-H]^-$	718.539	281.4	0.1	263.4
PE 35:2	$C_{40}H_{76}NO_8P$	$[M+H]^+$	730.538	297.8	0.1	274.0	$[M-H]^-$	728.523	280.9	0.1	262.9
PE 35:1	$C_{40}H_{78}NO_8P$	[M+H]+	732.553	300.3	0.1	276.0	[M-H]-	730.539	283.2	0.0	264.9
PE 36:2	$C_{41}H_{78}NO_8P$	$[M+H]^+$	744.553	298.8	0.1	274.8	$[M-H]^-$	742.539	284.6	0.1	266.2
PE 36:1	$C_{41}H_{80}NO_8P$	[M+H]+	746.569	304.4	0.1	279.3	[M-H]-	744.554	286.4	0.1	267.9

90

91

92

93

		Positive ions					Negative ions				
membrane lipids of PAK	**Formula**	**ion**	***m/z***	**$^{TW}CCS_{N2}$ without correction**	**$^{TW}CCS_{N2}$ %RSD**	**corrected $^{TW}CCS_{N2}$ (Å²)**	**ion**	***m/z***	**$^{TW}CCS_{N2}$ without correction**	**$^{TW}CCS_{N2}$ %RSD**	**corrected $^{TW}CCS_{N2}$ (Å²)**
PG 30:0	$C_{36}H_{71}O_{10}P$						[M-H]-	693.4712	275.8	0.1	258.3
PG 32:1	$C_{38}H_{71}O_{10}P$						$[M-H]^-$	719.4869	281.4	0.1	263.4
PG 33:1	$C_{39}H_{75}O_{10}P$						$[M-H]^-$	733.5025	283.5	0.1	265.3
PG 34:2	$C_{40}H_{75}O_{10}P$						$[M-H]^-$	745.5025	285.1	0.1	266.6
PG 34:1	$C_{40}H_{77}O_{10}P$						$[M-H]^-$	747.5182	287.1	0.1	268.5
PG 35:2	$C_{40}H_{75}O_{10}P$						$[M-H]^-$	759.5182	288.5	0.1	269.7
PG 35:1	$C_{40}H_{77}O_{10}P$						$[M-H]^-$	761.5338	290.2	0.1	271.3
PG 36:2	$C_{42}H_{79}O_{10}P$						$[M-H]^-$	773.5338	291.7	0.1	272.6
CL 66:3	$C_{75}H_{140}O_{17}P_2$	$[M+H]^+$	1375.963	441.0	0.2	390.1	$[M-H]^-$	1373.949	411.2	0.3	380.4
CL 66:2	$C_{75}H_{142}O_{17}P_2$	$[M+H]^+$	1377.979	442.3	0.0	391.2	$[M-H]^-$	1375.965	412.5	0.4	381.6
CL 66:1	$C_{75}H_{144}O_{17}P_2$	$[M+H]^+$	1379.995	443.2	0.1	391.9					
CL 67:3	$C_{76}H_{142}O_{17}P_2$	$[M+H]^+$	1389.979	444.4	0.2	392.8					
CL 67:2	$C_{76}H_{144}O_{17}P_2$	$[M+H]^+$	1391.995	445.4	0.2	393.7					
CL 68:4	$C_{77}H_{142}O_{17}P_2$	$[M+H]^+$	1401.979	445.8	0.2	394.0					
CL 68:3	$C_{77}H_{144}O_{17}P_2$	$[M+H]^+$	1403.995	447.9	0.1	395.7					
CL 68:2	$C_{77}H_{146}O_{17}P_2$	$[M+H]^+$	1406.010	450.1	0.2	397.4	$[M-H]^-$	1403.996	418.4	0.3	386.9
CL 69:4	$C_{78}H_{144}O_{17}P_2$	[M+H]+	1415.995	449.2	0.2	396.7					
CL 69:3	$C_{78}H_{146}O_{17}P_2$	$[M+H]^+$	1418.010	451.1	0.2	398.3					
CL 69:2	$C_{78}H_{148}O_{17}P_2$	$[M+H]^+$	1420.026	452.0	0.1	399.0					
CL 70:4	$C_{79}H_{146}O_{17}P_2$	[M+H]+	1430.010	452.4	0.1	399.4					
CL 70:3	$C_{79}H_{148}O_{17}P_2$	[M+H]+	1432.026	454.7	0.1	401.2					

94

95
96

Table S3 $^{TW}CCS_{N2}$ values calibrated with **polyalanine** for the membrane lipids of PAK

		Positive ions					Negative ions				
membrane lipids of PAK	**Formula**	**ion**	***m/z***	**$^{TW}CCS_{N2}$ without correction**	**$^{TW}CCS_{N2}$ %RSD**	**corrected $^{TW}CCS_{N2}$ (Å²)**	**ion**	***m/z***	**$^{TW}CCS_{N2}$ without correction**	**$^{TW}CCS_{N2}$ %RSD**	**corrected $^{TW}CCS_{N2}$ (Å²)**
PC 32:1	$C_{40}H_{78}NO_8P$	$[M+H]^+$	732.5538	291.9	0.1	278.9					
PC 32:0	$C_{40}H_{80}NO_8P$	$[M+H]^+$	734.5694	295.5	0.1	282.1					
PC 34:2	$C_{42}H_{82}NO_8P$	$[M+H]^+$	758.5694	295.4	0.1	282.0					
PC 34:1	$C_{42}H_{82}NO_8P$	$[M+H]^+$	760.5851	298.6	0.1	284.8					
PC 34:0	$C_{42}H_{84}NO_8P$	$[M+H]^+$	762.6007	301.6	0.4	287.4					
PC 35:1	$C_{43}H_{84}NO_8P$	[M+H]+	774.6007	303.5	0.1	289.1					
PC 36:2	$C_{42}H_{82}NO_8P$	$[M+H]^+$	786.6007	302.4	0.1	288.2					
PE 30:1	$C_{35}H_{68}NO_8P$	$[M+H]^+$	662.4755	270.9	0.1	260.4	$[M-H]^-$	660.4610	259.2	0.1	249.7
PE 30:0	$C_{35}H_{70}NO_8P$						$[M-H]^-$	662.4766	261.6	0.1	251.8
PE 32:2	$C_{37}H_{70}NO_8P$	$[M+H]^+$	688.4912	273.1	0.1	262.4	$[M-H]^-$	686.4766	263.8	0.2	253.7
PE 32:1	$C_{37}H_{72}NO_8P$	$[M+H]^+$	690.5068	277.8	0.1	266.5	$[M-H]^-$	688.4923	265.7	0.1	255.4
PE 32:0	$C_{37}H_{74}NO_8P$	$[M+H]^+$	692.5225	283.6	0.0	271.6	$[M-H]^-$	690.5079	267.6	0.1	257.1
PE 33:1	$C_{38}H_{74}NO_8P$	$[M+H]^+$	704.5225	283.2	0.1	271.2	$[M-H]^-$	702.5079	269.5	0.1	258.8
PE 34:2	$C_{39}H_{73}NO_8P$	$[M+H]^+$	716.5225	280.6	0.1	269.0	$[M-H]^-$	714.5079	270.9	0.1	260.0
PE 34:1	$C_{37}H_{76}NO_8P$	$[M+H]^+$	718.5381	285.9	0.1	273.6	$[M-H]^-$	716.5236	272.8	0.0	261.7
PE 34:0	$C_{39}H_{78}NO_8P$	$[M+H]^+$	720.5538	289.5	0.1	276.8	$[M-H]^-$	718.5392	274.8	0.1	263.4
PE 35:2	$C_{40}H_{76}NO_8P$	$[M+H]^+$	730.5381	286.5	0.1	274.2	$[M-H]^-$	728.5236	274.2	0.1	262.9
PE 35:1	$C_{40}H_{78}NO_8P$	[M+H]+	732.5538	288.8	0.1	276.2	[M-H]-	730.5392	276.6	0.0	265.0
PE 36:2	$C_{41}H_{78}NO_8P$	$[M+H]^+$	744.5538	287.4	0.1	274.9	$[M-H]^-$	742.5392	278.0	0.2	266.3
PE 36:1	$C_{41}H_{80}NO_8P$	[M+H]+	746.5694	292.5	0.1	279.5	[M-H]-	744.5549	279.9	0.1	267.9

101

		Positive ions					Negative ions				
membrane lipids of PAK	**Formula**	**ion**	***m/z***	**$^{TW}CCS_{N2}$ without correction**	**$^{TW}CCS_{N2}$ %RSD**	**corrected $^{TW}CCS_{N2}$ (Å²)**	**ion**	***m/z***	**$^{TW}CCS_{N2}$ without correction**	**$^{TW}CCS_{N2}$ %RSD**	**corrected $^{TW}CCS_{N2}$ (Å²)**
PG 30:0	$C_{36}H_{71}O_{10}P$						[M-H]-	693.4712	269.0	0.1	258.3
PG 32:1	$C_{38}H_{71}O_{10}P$						$[M-H]^-$	719.4869	274.8	0.1	263.4
PG 33:1	$C_{39}H_{75}O_{10}P$						$[M-H]^-$	733.5025	276.9	0.1	265.3
PG 34:2	$C_{40}H_{75}O_{10}P$						$[M-H]^-$	745.5025	278.5	0.1	266.7
PG 34:1	$C_{40}H_{77}O_{10}P$						$[M-H]^-$	747.5182	280.6	0.1	268.6
PG 35:2	$C_{40}H_{75}O_{10}P$						$[M-H]^-$	759.5182	282.0	0.1	269.8
PG 35:1	$C_{40}H_{77}O_{10}P$						$[M-H]^-$	761.5338	283.8	0.1	271.4
PG 36:2	$C_{42}H_{79}O_{10}P$						$[M-H]^-$	773.5338	285.3	0.1	272.7
CL 66:3	$C_{75}H_{140}O_{17}P_2$	$[M+H]^+$	1375.9639	416.5	0.2	388.9	$[M-H]^-$	1373.9493	409.5	0.3	382.4
CL 66:2	$C_{75}H_{142}O_{17}P_2$	$[M+H]^+$	1377.9795	417.7	0.0	389.9	$[M-H]^-$	1375.9650	410.9	0.4	383.6
CL 66:1	$C_{75}H_{144}O_{17}P_2$	$[M+H]^+$	1379.9952	418.6	0.1	390.6					
CL 67:3	$C_{76}H_{142}O_{17}P_2$	$[M+H]^+$	1389.9795	419.6	0.2	391.5					
CL 67:2	$C_{76}H_{144}O_{17}P_2$	$[M+H]^+$	1391.9952	420.6	0.1	392.4					
CL 68:4	$C_{77}H_{142}O_{17}P_2$	$[M+H]^+$	1401.9795	420.9	0.2	392.7					
CL 68:3	$C_{77}H_{144}O_{17}P_2$	$[M+H]^+$	1403.9952	422.8	0.1	394.4					
CL 68:2	$C_{77}H_{146}O_{17}P_2$	$[M+H]^+$	1406.0108	424.7	0.2	396.1	$[M-H]^-$	1403.9963	417.0	0.3	389.1
CL 69:4	$C_{78}H_{144}O_{17}P_2$	[M+H]+	1415.9952	423.9	0.2	395.4					
CL 69:3	$C_{78}H_{146}O_{17}P_2$	$[M+H]^+$	1418.0108	425.6	0.2	396.9					
CL 69:2	$C_{78}H_{148}O_{17}P_2$	$[M+H]^+$	1420.0265	426.5	0.1	397.6					
CL 70:4	$C_{79}H_{146}O_{17}P_2$	[M+H]+	1430.0108	426.8	0.1	398.0					
CL 70:3	$C_{79}H_{148}O_{17}P_2$	[M+H]+	1432.0265	428.8	0.1	399.7					

102

103
104

105

Table S4 $^{TW}CCS_{N2}$ values calibrated with **phospholipids** for the membrane lipids of PAK

		Positive ions				Negative ions			
membrane lipids of PAK	**Formula**	**ion**	***m/z***	**$^{TW}CCS_{N2}$ without correction (Å²)**	**$^{TW}CCS_{N2}$ %RSD**	**ion**	***m/z***	**$^{TW}CCS_{N2}$ without correction**	**$^{TW}CCS_{N2}$ %RSD**
PC 32:1	$C_{40}H_{78}NO_8P$	$[M+H]^+$	732.5538	279.0	0.1				
PC 32:0	$C_{40}H_{80}NO_8P$	$[M+H]^+$	734.5694	282.2	0.1				
PC 34:2	$C_{42}H_{82}NO_8P$	$[M+H]^+$	758.5694	282.1	0.1				
PC 34:1	$C_{42}H_{82}NO_8P$	$[M+H]^+$	760.5851	284.9	0.1				
PC 34:0	$C_{42}H_{84}NO_8P$	$[M+H]^+$	762.6007	287.4	0.3				
PC 35:1	$C_{43}H_{84}NO_8P$	[M+H]+	774.6007	289.1	0.1				
PC 36:2	$C_{42}H_{82}NO_8P$	$[M+H]^+$	786.6007	288.2	0.1				
PE 30:1	$C_{35}H_{68}NO_8P$	$[M+H]^+$	662.4755	260.8	0.1	$[M-H]^-$	660.4610	253.9	0.1
PE 30:0	$C_{35}H_{70}NO_8P$					$[M-H]^-$	662.4766	256.0	0.1
PE 32:2	$C_{37}H_{70}NO_8P$	$[M+H]^+$	688.4912	262.7	0.1	$[M-H]^-$	686.4766	257.9	0.2
PE 32:1	$C_{37}H_{72}NO_8P$	$[M+H]^+$	690.5068	266.8	0.1	$[M-H]^-$	688.4923	259.5	0.1
PE 32:0	$C_{37}H_{74}NO_8P$	$[M+H]^+$	692.5225	271.8	0.0	$[M-H]^-$	690.5079	261.2	0.1
PE 33:1	$C_{38}H_{74}NO_8P$	$[M+H]^+$	704.5225	271.5	0.1	$[M-H]^-$	702.5079	262.9	0.1
PE 34:2	$C_{39}H_{73}NO_8P$	$[M+H]^+$	716.5225	269.2	0.1	$[M-H]^-$	714.5079	264.1	0.1
PE 34:1	$C_{37}H_{76}NO_8P$	$[M+H]^+$	718.5381	273.8	0.1	$[M-H]^-$	716.5236	265.7	0.0
PE 34:0	$C_{39}H_{78}NO_8P$	$[M+H]^+$	720.5538	277.0	0.1	$[M-H]^-$	718.5392	267.4	0.1
PE 35:2	$C_{40}H_{76}NO_8P$	$[M+H]^+$	730.5381	274.4	0.1	$[M-H]^-$	728.5236	266.9	0.1
PE 35:1	$C_{40}H_{78}NO_8P$	[M+H]+	732.5538	276.4	0.1	[M-H]-	730.5392	269.0	0.0
PE 36:2	$C_{41}H_{78}NO_8P$	$[M+H]^+$	744.5538	275.1	0.1	$[M-H]^-$	742.5392	270.2	0.1
PE 36:1	$C_{41}H_{80}NO_8P$	[M+H]+	746.5694	279.6	0.1	[M-H]-	744.5549	271.8	0.1

551

106

107

108

		Positive ions				Negative ions			
membrane lipids of PAK	**Formula**	**ion**	***m/z***	**$^{TW}CCS_{N2}$ without correction (Å²)**	**$^{TW}CCS_{N2}$ %RSD**	**corrected $^{TW}CCS_{N2}$ (Å²)**	**ion**	***m/z***	**$^{TW}CCS_{N2}$ without correction (Å²)**
PG 30:0	$C_{36}H_{71}O_{10}P$					[M-H]-	693.4712	262.4	0.1
PG 32:1	$C_{38}H_{71}O_{10}P$					$[M-H]^-$	719.4869	267.4	0.1
PG 33:1	$C_{39}H_{75}O_{10}P$					$[M-H]^-$	733.5025	269.3	0.1
PG 34:2	$C_{40}H_{75}O_{10}P$					$[M-H]^-$	745.5025	270.6	0.1
PG 34:1	$C_{40}H_{77}O_{10}P$					$[M-H]^-$	747.5182	272.5	0.1
PG 35:2	$C_{40}H_{75}O_{10}P$					$[M-H]^-$	759.5182	273.7	0.1
PG 35:1	$C_{40}H_{77}O_{10}P$					$[M-H]^-$	761.5338	275.3	0.1
PG 36:2	$C_{42}H_{79}O_{10}P$					$[M-H]^-$	773.5338	276.5	0.1
CL 66:3	$C_{75}H_{140}O_{17}P_2$	$[M+H]^+$	1375.963	385.4	0.2	$[M-H]^-$	1373.9493	381.4	0.3
CL 66:2	$C_{75}H_{142}O_{17}P_2$	$[M+H]^+$	1377.979	386.4	0.0	$[M-H]^-$	1375.9650	382.6	0.4
CL 66:1	$C_{75}H_{144}O_{17}P_2$	$[M+H]^+$	1379.995	387.1	0.1				
CL 67:3	$C_{76}H_{142}O_{17}P_2$	$[M+H]^+$	1389.979	387.9	0.2				
CL 67:2	$C_{76}H_{144}O_{17}P_2$	$[M+H]^+$	1391.995	388.8	0.1				
CL 68:4	$C_{77}H_{142}O_{17}P_2$	$[M+H]^+$	1401.979	389.0	0.2				
CL 68:3	$C_{77}H_{144}O_{17}P_2$	$[M+H]^+$	1403.995	390.6	0.1				
CL 68:2	$C_{77}H_{146}O_{17}P_2$	$[M+H]^+$	1406.010	392.2	0.1	$[M-H]^-$	1403.9963	387.7	0.3
CL 69:4	$C_{78}H_{144}O_{17}P_2$	[M+H]+	1415.995	391.6	0.1				
CL 69:3	$C_{78}H_{146}O_{17}P_2$	$[M+H]^+$	1418.010	393.0	0.2				
CL 69:2	$C_{78}H_{148}O_{17}P_2$	$[M+H]^+$	1420.026	393.7	0.1				
CL 70:4	$C_{79}H_{146}O_{17}P_2$	[M+H]+	1430.010	394.0	0.1				
CL 70:3	$C_{79}H_{148}O_{17}P_2$	[M+H]+	1432.026	395.8	0.1				

Table S5 Comparison between the experimental $^{TW}CCS_{N2}$ values for the phospholipids of PAK and CCS values of the literature for $[M+H]^+$. 1: dextran calibration, 2: dextran calibration and lipid correction, 3: polyalanine calibration, 4: polyalanine calibration and lipid correction, 5 phospholipids calibration

	Leaptrot 2019 - drift tube						Zhou 2017 - drift tube						Hines 2016 - drift tube						Paglia 2015 - TWIMS polyalanine calibration					
Lipid	**CCS [M+H]+ (Å²)**	**% Δ 1**	**% Δ 2**	**% Δ 3**	**% Δ 4**	**% Δ 5**	**CCS [M+H]+ (Å²)**	**% Δ 1**	**% Δ 2**	**% Δ 3**	**% Δ 4**	**% Δ 5**	**CCS [M+H]+ (Å²)**	**% Δ 1**	**% Δ 2**	**% Δ 3**	**% Δ 4**	**% Δ 5**	**CCS [M+H]+ (Å²)**	**% Δ 1**	**% Δ 2**	**% Δ 3**	**% Δ 4**	**% Δ 5**
PC 32:0	278.4	10.5	1.3	6.0	1.3	1.4	283.4	8.5	-0.5	4.1	-0.5	-0.4	282.5	8.9	-0.2	4.4	-0.1	-0.1	291.0	5.7	-3.1	1.4	-3.1	-3.0
PC 32:1	276.5	9.8	0.8	5.6	0.9	0.9	282.6	7.4	-1.4	3.3	-1.3	-1.3							287.0	5.8	-2.9	1.7	-2.8	-2.8
PC 34:0							289.7	8.5	-0.8	4.1	-0.8	-0.8							297.0	5.8	-3.3	1.5	-3.2	-3.2
PC 34:1	282.0	10.3	1.0	5.9	1.0	1.0	287.1	8.3	-0.8	4.0	-0.8	-0.8							295.0	5.4	-3.5	1.2	-3.5	-3.4
PC 34:2	279.5	10.0	0.9	5.7	1.9	1.9	285.2	7.8	-1.2	3.6	-0.1	-0.1							293.0	4.9	-3.8	0.8	-2.8	-2.8
PC 35:1	287.1	10.2	0.7	5.7	0.7	0.7	289.2	9.4	-0.1	4.9	0.0	0.0												
PC 36:2	288.6	9.2	-0.2	4.8	-0.1	-0.1	291.3	8.2	-1.1	3.8	-1.1	-1.1							301.0	4.7	-4.3	0.5	-4.3	-4.3
PE 32:0							271.4	8.5	0.0	4.5	0.1	0.1	271.5	8.5	0.0	4.5	0.0	0.1						
PE 32:1							267.2	7.9	-0.3	4.0	-0.3	-0.2												
PE 32:2													263.8	7.4	-0.6	3.5	-0.5	-0.4						
PE 34:0							277.5	8.5	-0.3	4.3	-0.3	-0.2	277.4	8.5	-0.3	4.4	-0.2	-0.1						
PE 34:1	270.1	10.0	1.2	5.9	1.3	1.4	274.7	8.2	-0.5	4.1	-0.4	-0.3	273.4	8.7	0.0	4.6	0.1	0.1	272.0	9.2	0.5	5.1	0.6	0.7
PE 34:2	268.5	8.5	0.1	4.5	0.2	0.3	272.7	6.8	-1.4	2.9	-1.4	-1.3												
PE 35:1							276.6	8.6	-0.2	4.4	-0.1	-0.1												
PE 35:2							275.0	8.3	-0.4	4.2	-0.3	-0.2												
PE 36:1	277.0	9.9	0.8	5.6	0.9	0.9	281.3	8.2	-0.7	4.0	-0.7	-0.6												
PE 36:2	275.1	8.6	-0.1	4.5	-0.1	0.0	279.3	7.0	-1.6	2.9	-1.6	-1.5	277.9	7.5	-1.1	3.4	-1.1	-1.0	279.0	7.1	-1.5	3.0	-1.5	-1.4

Table S6 Comparison between the experimental $^{TW}CCS_{N2}$ values for the phospholipids of PAK and CCS values of the literature for $[M-H]^-$.

117

1: dextran calibration, 2: dextran calibration and lipid correction, 3: polyalanine calibration, 4: polyalanine calibration and lipid correction, 5 phospholipids calibration

	Leaptrot 2019 - drift tube						Zhou 2017 - drift tube						Hines 2016 - drift tube						Paglia 2015 - TWIMS polyalanine calibration					
Lipid	**CCS $[M-H]^-$ (Å²)**	**% Δ 1**	**% Δ 2**	**% Δ 3**	**% Δ 4**	**% Δ 5**	**CCS $[M-H]^-$ (Å²)**	**% Δ 1**	**% Δ 2**	**% Δ 3**	**% Δ 4**	**% Δ 5**	**CCS $[M-H]^-$ (Å²)**	**% Δ 1**	**% Δ 2**	**% Δ 3**	**% Δ 4**	**% Δ 5**	**CCS $[M-H]^-$ (Å²)**	**% Δ 1**	**% Δ 2**	**% Δ 3**	**% Δ 4**	**% Δ 5**
PE(30:0)													253.3	6.0	-1.4	2.3	-1.4	0.2						
PE(32:1)							256.6	6.2	-0.5	3.5	-0.5	1.1												
PE(32:0)													259.4	5.8	-0.9	3.2	-0.9	0.7						
PE(32:2)													256.3	5.6	-1.0	2.9	-1.0	0.6						
PE(34:0)													265.5	6.0	-0.8	3.5	-0.8	0.7	274	2.7	-3.9	0.3	-3.9	-2.4
PE(34:1)	266.9	4.7	-2.0	2.2	-2.0	-0.5	263.1	6.2	-0.6	3.7	-0.5	1.0	264.5	5.7	-1.1	3.1	-1.1	0.5						
PE(34:2)	265.6	4.6	-2.1	2.0	-2.1	-0.6																		
PE(36:1)	273.6	4.7	-2.1	2.3	-2.1	-0.7																		
PE(36:2)	272.1	4.6	-2.2	2.2	-2.1	-0.7	268.5	6.0	-0.9	3.5	-0.8	0.6	270.7	5.1	-1.7	2.7	-1.6	-0.2						
PG(32:1)							263.3	6.9	0.0	4.4	0.0	1.6												
PG(33:1)							266.4	6.4	-0.4	4.0	-0.4	1.1												
PG(34:0)																			283	2.0	-4.7	-0.3	-4.6	-3.3
PG(34:1)							270.2	6.3	-0.6	3.8	-0.6	0.9							281	2.2	-4.4	-0.1	-4.4	-3.0
PG(34:2)							268.7	6.1	-0.8	3.6	-0.7	0.7							279	2.2	-4.4	-0.2	-4.4	-3.0
PG(35:1)							272.7	6.4	-0.5	4.1	-0.5	0.9												
PG(36:2)																			289	0.9	-5.7	-1.3	-5.6	-4.3

118

119

120

Table S7: ΔCCS (%) comparison between CCS values of the literature for $[M+H]^+$

Lipid	Leaptrot / Zhou	Leaptrot / Hines	Zhou / Hines	Zhou / Paglia	Hines / Paglia
PC(32:0)	-1.8	-1.5	0.3	-2.6	-2.9
PC(32:1)	-2.2			-1.5	
PC(34:0)				-2.5	
PC(34:1)	-1.8			-2.7	
PC(34:2)	-2.0			-2.7	
PC(36:2)	-0.9			-3.2	
PE(32:0)			0.0		
PE(34:0)			0.0		
PE(34:1)	-1.7	-1.2	0.5	1.0	0.5
PE(36:2)	-1.5	-1.0	0.5	0.1	-0.4

Table S8: ΔCCS (%) comparison between CCS values of the literature for $[M-H]^-$

	Δ Comparison between the literature (%)			
Lipid	Leaptrot / Zhou	Leaptrot / Hines	Zhou / Hines	Zhou / Paglia
PE(34:1)	1.4	0.9	-0.5	
PE(36:2)	1.3	0.5	-0.8	
PG(34:1)				-3.8
PG(34:2)				-3.7

The following figure describes the ***$^{TW}CCS_{N2}$ vs m/z correlation***

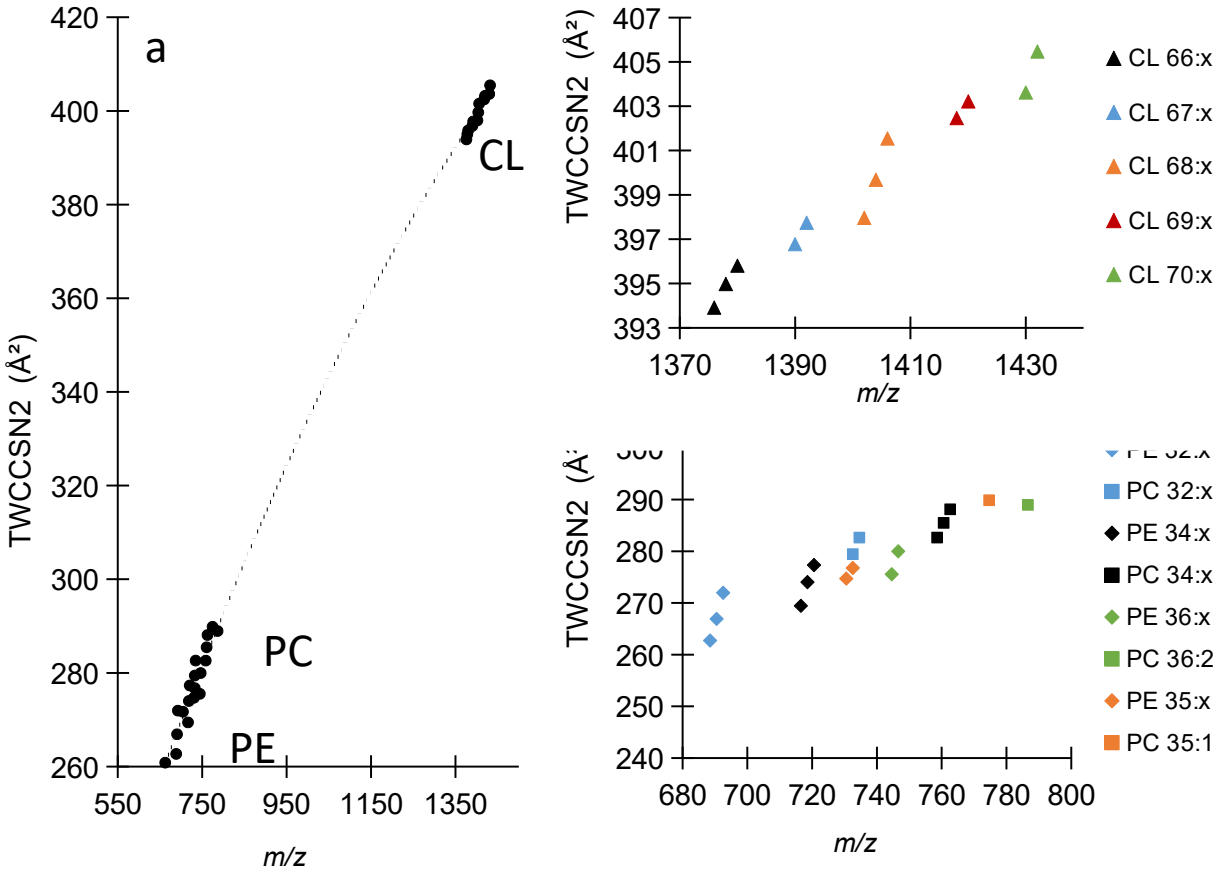

Figure S9: $^{TW}CCS_{N2}$ values plotted against *m/z* for positive ions. (a) represents values for every class of phospholipids, whereas (b) only represents values for CLs and (c) only represents values for PCs and PEs. CLs are represented by triangles, PCs are represented by squares, PEs by diamonds. x refers to the number of double-bonds on the fatty acid moiety of the phospholipid which can be equal to 0, 1, 2 (for PCs and PEs) or up to 3, 4 (for CLs).

S2 Dextran, polyalanine and phospholipids CCS Calibration

Positive Dextran Calibration

M(N2) 28.0134

Glc_n		m/z	z	m	CCS (N_2) in Å²	1/μ	Ω'(N2) litt	td	ln(Ω'(N2))	ln(td)		
2	$[M+Na]^+$	365.11	1	365.11	179.54	0.04	915.77	2.28	6.82	0.82		
3	$[M+Na]^+$	527.16	1	527.16	215.00	0.04	1108.88	3.21	7.01	1.17		
4	$[M+Na]^+$	689.21	1	689.21	243.36	0.04	1262.66	4.01	7.14	1.39		
5	$[M+Na]^+$	851.26	1	851.26	273.81	0.04	1425.94	4.89	7.26	1.59		
6	$[M+Na]^+$	1013.32	1	1013.32	302.06	0.04	1577.08	5.75	7.36	1.75	x	0.590
7	$[M+Na]^+$	1175.37	1	1175.37	330.94	0.04	1731.10	6.74	7.46	1.91	lnA	6.328
8	$[M+Na]^+$	1337.42	1	1337.42	355.80	0.04	1863.77	7.68	7.53	2.04	A	560.026
9	$[M+Na]^+$	1499.48	1	1499.48	377.70	0.04	1980.68	8.53	7.59	2.14	r^2	0.9998

Positive Polyalanine Calibration

M(N2) 28.0134

Sequenz	m/z	z	m	CCS (N_2) in Å²	1/μ	Ω'(N2) litt	td	ln(Ω'(N2))	ln(td)		
A4	303.208	1	303.2	166.00	0.04	840.62	2.06	6.73	0.72		
A5	374.208	1	374.2	181.00	0.04	924.03	2.42	6.83	0.88		
A6	445.208	1	445.2	195.00	0.04	1001.08	2.76	6.91	1.02		
A7	516.308	1	516.3	211.00	0.04	1087.66	3.17	6.99	1.15	x	0.563
A8	587.308	1	587.3	228.00	0.04	1178.96	3.67	7.07	1.30	lnA	6.336
A9	658.308	1	658.3	243.00	0.04	1259.62	4.12	7.14	1.42	A	564.400
A10	729.408	1	729.4	256.00	0.04	1329.66	4.54	7.19	1.51	r^2	0.9991
A11	800.408	1	800.4	271.00	0.04	1409.88	5.01	7.25	1.61		
A12	871.508	1	871.5	282.00	0.04	1469.14	5.50	7.29	1.70		
A13	942.508	1	942.5	294.00	0.04	1533.45	5.98	7.34	1.79		
A14	1013.508	1	1013.5	306.00	0.04	1597.66	6.45	7.38	1.86		

Positive Lipids Calibration

M(N2) 28.0134

Lipide	m/z	z	m	CCS (N_2) in Å²	1/μ	Ω'(N2) litt	td	ln(Ω'(N2))	ln(td)		
PE 6:0/6:0	412.2095	1	412.2095	202.1	0.04	1035.08	2.94	6.94	1.08		
PE 10:0/10:0	524.3347	1	524.3347	233	0.04	1201.54	4.06	7.09	1.40		
PE 15:0/15:0	664.4912	1	664.4912	265	0.04	1373.92	5.30	7.23	1.67	x	0.512
PE 17:0/17:0	720.5538	1	720.5538	277.4	0.04	1440.48	5.76	7.27	1.75	lnA	6.380
PC 20:0/20:0	846.6946	1	846.6946	306.4	0.04	1595.52	6.96	7.37	1.94	A	590.169
PC 24:0/24:0	958.8198	1	958.8198	330.9	0.04	1726.34	7.98	7.45	2.08	r^2	0.9981

137

Negative Dextran Calibration

M(N2) 28.0134

Glc_n		m/z	z	m	CCS (N_2) in Å²	1/μ	Ω'(N2) litt	td	ln(Ω'(N2))	ln(td)		
2	$[M-H]^-$	341.11	1	341.11	174.56	0.04	888.17	2.02	6.79	0.70		
3	$[M-H]^-$	503.16	1	503.16	202.34	0.04	1042.30	3.03	6.95	1.11		
4	$[M-H]^-$	665.21	1	665.21	233.96	0.04	1213.00	3.92	7.10	1.37		
5	$[M-H]^-$	827.27	1	827.27	265.39	0.04	1381.45	4.86	7.23	1.58		
6	$[M-H]^-$	989.32	1	989.32	296.73	0.04	1548.76	5.85	7.35	1.77	x	0.546
7	$[M-H]^-$	1151.37	1	1151.37	319.21	0.04	1669.34	6.71	7.42	1.90	lnA	6.374
8	$[M-H]^-$	1313.43	1	1313.43	343.55	0.04	1799.25	7.71	7.50	2.04	A	586.226
9	$[M-H]^-$	1475.48	1	1475.48	365.21	0.04	1914.89	8.64	7.56	2.16	r^2	0.9953

Negative Polyalanine Calibration

M(N2) 28.0134

Sequenz	m/z	z	m	CCS (N_2) in Å²	1/μ	Ω'(N2) litt	td	ln(Ω'(N2))	ln(td)		
A4	301.151	1	301.2	165.00	0.04	835.32	2.09	6.73	0.74		
A5	372.188	1	372.2	179.00	0.04	913.65	2.48	6.82	0.91		
A6	443.225	1	443.2	195.00	0.04	1000.94	2.86	6.91	1.05		
A7	514.262	1	514.3	209.00	0.04	1077.24	3.28	6.98	1.19	x	0.576
A8	585.300	1	585.3	223.00	0.04	1153.02	3.67	7.05	1.30	lnA	6.301
A9	656.337	1	656.3	238.00	0.04	1233.63	4.12	7.12	1.42	A	545.101
A10	727.374	1	727.4	253.00	0.04	1314.01	4.58	7.18	1.52	r^2	0.9998
A11	798.411	1	798.4	267.00	0.04	1389.01	5.06	7.24	1.62		
A12	869.448	1	869.4	279.00	0.04	1453.45	5.50	7.28	1.70		
A13	940.485	1	940.5	294.00	0.04	1533.40	6.04	7.34	1.80		
A14	1011.522	1	1011.5	308.00	0.04	1608.06	6.58	7.38	1.88		

Negative Lipids Calibration

M(N2) 28.0134

Lipide	m/z	z	m	CCS (N_2) in Å²	1/μ	Ω'(N2) litt	td	ln(Ω'(N2))	ln(td)		
PE 6:0/6:0	410.1949	1	410.1949	199.3	0.04	1020.58	3.03	6.93	1.10		
PE 10:0/10:0	522.3201	1	522.3201	223.2	0.04	1150.89	3.85	7.05	1.34		
PE 15:0/15:0	662.4766	1	662.4766	253.3	0.04	1313.18	4.92	7.18	1.59	x	0.517
PE 17:0/17:0	718.5392	1	718.5392	265.5	0.04	1378.61	5.39	7.23	1.68	lnA	6.359
PC 20:0/20:0	904.7012	1	904.7012	305.1	0.04	1590.39	7.15	7.37	1.96	A	577.820
PC 24:0/24:0	1016.8264	1	1016.8264	331	0.04					r^2	0.9998

[M+CH3COO-]

565
138

139
140

141

566 **S3 Dextran and polyalanine correction curves**

Positive values — Measured with dextran calibration

Lipids	m/z	z	td	td'	CCS' (N2)	$^{TW}CCS_{N2}$	$^{DT}CCS_{N2}$ lit.	Ω %Δ
PE 6:0/6:0	412.210	1	2.94	2.91	1058.4	206.7	202.1	2.3
PE 10:0/10:0	524.335	1	4.06	4.02	1280.7	248.4	233.0	-6.6
PE 15:0/15:0	664.491	1	5.30	5.26	1498.7	289.1	265.0	-9.1
PE 17:0/17:0	720.554	1	5.76	5.72	1574.0	303.1	277.4	-9.3
PC 20:0/20:0	846.695	1	6.96	6.91	1759.8	337.9	306.4	-10.3
PC 24:0/24:0	958.820	1	7.98	7.93	1907.4	365.6	330.9	-10.5

Equation A: lipid standards positive correction

a	0.8107
b	32.5654
r^2	0.9988

correction curve for dextran calibration in positive mode

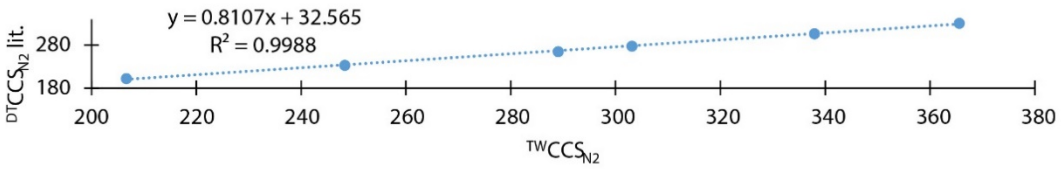

Negative values — Measured with dextran calibration

Lipids	m/z	z	td	td'	CCS' (N2)	$^{TW}CCS_{N2}$	$^{DT}CCS_{N2}$ lit.	Ω %Δ
PE 6:0/6:0	410.195	1	3.03	3.00	1075.0	209.9	199.3	5.3
PE 10:0/10:0	522.320	1	3.85	3.81	1225.3	237.6	223.2	-6.5
PE 15:0/15:0	662.477	1	4.92	4.88	1400.8	270.2	253.3	-6.7
PE 17:0/17:0	718.539	1	5.39	5.35	1472.4	283.6	265.5	-6.8
PC 20:0/20:0	904.701	1						
PC 24:0/24:0	1016.826	1						

Equation B: lipid standards negative correction

a	0.9018
b	9.5704
r^2	0.9998

correction curve for dextran calibration in negative mode

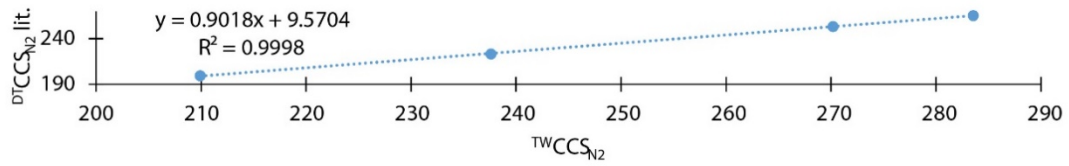

567

142

143

144

Positive values

Measured with polyalanine calibration

Lipids	m/z	z	td	td'	CCS' (N_2)	$^{TW}CCS_{N2}$	$^{DT}CCS_{N2}$ lit.	Ω %Δ
PE 6:0/6:0	412.210	1	2.94	2.91	1036.1	202.3	202.1	2.3
PE 10:0/10:0	524.335	1	4.06	4.02	1242.9	241.0	233.0	-6.6
PE 15:0/15:0	664.491	1	5.30	5.26	1444.0	278.5	265.0	-9.1
PE 17:0/17:0	720.554	1	5.76	5.72	1513.2	291.4	277.4	-9.3
PC 20:0/20:0	846.695	1	6.96	6.91	1683.1	323.2	306.4	-10.3
PC 24:0/24:0	958.820	1	7.98	7.93	1817.5	348.4	330.9	-10.5

correction curve for polyalanine calibration in positive mode

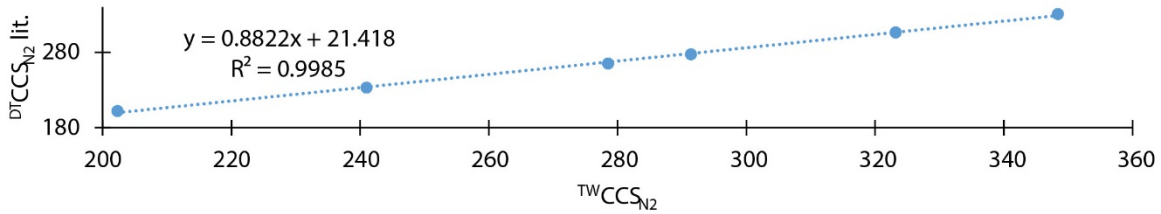

Negative values

Measured with polyalanine calibration

Lipids	m/z	z	td	td'	CCS' (N_2)	$^{TW}CCS_{N2}$	$^{DT}CCS_{N2}$ lit.	Ω %Δ
PE 6:0/6:0	410.195	1	3.03	3.00	1033.2	201.8	199.3	5.3
PE 10:0/10:0	522.320	1	3.85	3.81	1185.5	229.9	223.2	-6.5
PE 15:0/15:0	662.477	1	4.92	4.88	1364.7	263.2	253.3	-6.7
PE 17:0/17:0	718.539	1	5.39	5.35	1438.1	276.9	265.5	-6.8
PC 20:0/20:0	904.701	1						
PC 24:0/24:0	1016.826	1						

correction curve for polyalanine calibration in negative mode